

Longitudinal flow from 2 to 8 AGeV Au+Au Collisions at the Brookhaven AGS

J.L. Klay⁽¹⁾, N.N. Ajitanand⁽²⁾, J.M. Alexander⁽²⁾, M.G. Anderson⁽¹⁾, D. Best⁽⁴⁾, F.P. Brady⁽¹⁾, T. Case⁽⁴⁾, W. Caskey⁽¹⁾, D. Cebra⁽¹⁾, J.L. Chance⁽¹⁾, P. Chung⁽²⁾, B. Cole⁽⁹⁾, K. Crowe⁽⁴⁾, A.C. Das⁽⁶⁾, J.E. Draper⁽¹⁾, M.L. Gilkes⁽⁵⁾, S. Gushue⁽⁸⁾, M. Heffner⁽¹⁾, A.S. Hirsch⁽⁵⁾, E.L. Hjort⁽⁵⁾, L. Huo⁽¹⁰⁾, M. Justice⁽³⁾, M. Kaplan⁽⁷⁾, D. Keane⁽³⁾, J.C. Kintner⁽¹²⁾, D. Krfccheck⁽¹¹⁾, R.A. Lacey⁽²⁾, J. Lauret⁽²⁾, C. Law⁽²⁾, M.A. Lisa⁽⁶⁾, H. Liu⁽³⁾, Y.M. Liu⁽¹⁰⁾, R. McGrath⁽²⁾, Z. Milosevich⁽⁷⁾, G. Odyniec⁽⁴⁾, D.L. Olson⁽⁴⁾, S.Y. Panitkin⁽³⁾, C. Pinkenburg⁽²⁾, N.T. Porile⁽⁵⁾, G. Rai⁽⁴⁾, H.G. Ritter⁽⁴⁾, J.L. Romero⁽¹⁾, R. Scharenberg⁽⁵⁾, L. Schroeder⁽⁴⁾, B. Srivastava⁽⁵⁾, N.T.B. Stone⁽⁴⁾, T.J.M. Symons⁽⁴⁾, S. Wang⁽³⁾, R. Wells⁽⁶⁾, J. Whitfield⁽⁷⁾, T. Wienold⁽⁴⁾, R. Witt⁽³⁾, L. Wood⁽¹⁾, and W.N. Zhang⁽¹⁰⁾
(E895 Collaboration)

⁽¹⁾University of California, Davis, California 95616

⁽²⁾Department of Chemistry and Physics, SUNY, Stony Brook, New York 11794-3400

⁽³⁾Kent State University, Kent, Ohio 44242

⁽⁴⁾Lawrence Berkeley National Laboratory, Berkeley, California 94720

⁽⁵⁾Purdue University, West Lafayette, Indiana, 47907-1396

⁽⁶⁾The Ohio State University, Columbus, Ohio 43210

⁽⁷⁾Carnegie Mellon University, Pittsburgh, Pennsylvania 15213

⁽⁸⁾Brookhaven National Laboratory, Upton, New York 11973

⁽⁹⁾Columbia University, New York, New York 10027

⁽¹⁰⁾Harbin Institute of Technology, Harbin, 150001 People's Republic of China

⁽¹¹⁾University of Auckland, Auckland, New Zealand

⁽¹²⁾St. Mary's College of California, Moraga, California 94575

(November 9, 2018)

Abstract

Longitudinal flow extracted from the rapidity density distributions of protons from $^{197}\text{Au} + ^{197}\text{Au}$ collisions measured by the E895 Collaboration in the energy range from 2 to 8 AGeV at the Brookhaven AGS is presented. The almost 4π coverage provided by the EOS Time Projection Chamber allows reconstruction of proton transverse mass spectra over a broad range of rapidities. The asymptotic slope of each $m_t - m_0$ spectrum provides a temperature with which to calculate an expected dN/dy using a thermal model which includes collective longitudinal flow. This expected dN/dy is fit to the data to extract the longitudinal flow. The results show an approximately linear increase in the longitudinal flow velocity, $\langle\beta\gamma\rangle_L$, as a function of the logarithm

of beam energy.

PACS numbers: 25.75.-q, 25.60.Gc, 25.75.Ld

Experimental heavy ion programs from the beam energy regime of the Bevalac and SIS to the AGS and the CERN SPS have attempted to characterize the final state distributions of particles emerging from high energy collisions in terms of simple thermodynamic principles. Testing the underlying assumptions of chemical and thermal equilibrations at different stages of the collision has been attempted by comparing model expectations to many different experimental observables. Static isotropic thermal emission models applied to observed particle rapidity density distributions from experiments at all beam energies consistently fail to describe the observed shape; such model predictions are always too narrow. In contrast, thermal models which include collective longitudinal expansion have been much more successful at reproducing the observed rapidity density distributions. [1,2] The additional collective motion is attributed to intense pressure gradients which develop in the very hot, compressed nuclear matter fireballs created in heavy ion collisions. The gradients, and therefore the expansion, need not be isotropic, however the cylindrical symmetry of central collisions at very small impact parameter suggests that the longitudinal and transverse components of any flow can be factorized.

At the AGS, rapidity density distributions of multiple particle species, including pions, kaons, protons and lambda hyperons have been simultaneously described by a thermal distribution with a common longitudinal collective expansion velocity. [3,2] The agreement between the proton and other mass particle distributions suggests nearly complete stopping of the incident nucleons at the top AGS energy, which implies even more complete stopping at the present beam energies. In contrast, for extremely high beam energies, Bjorken proposed [4] that nuclear transparency would evacuate the central rapidity region of all of the initial nucleons, leaving a hot, high-energy density region in which a Quark Gluon Plasma might form. In 160 AGeV Pb+Pb collisions at the CERN SPS, observed net proton ((+)-(-)) rapidity density distributions [5] exhibit a double-humped character which is not inconsistent with the onset of this transparency. At these higher energies, the nucleon distributions may not be describable by a simple thermal model with collective longitudinal flow, but rather need additional theoretical consideration of transparency. However, the negative hadron (mostly pions) rapidity distributions are well-described by this model, demonstrating a significant amount of collective longitudinal flow. [2]

More recently, models which attempt simultaneously to characterize many of the freeze-out parameters (transverse and longitudinal flow, temperature, chemical potential and source volume) have been attempted on data at and above the top energy at the AGS. [6] The data presented in this letter are compared only to the thermal model with longitudinal flow in order to directly compare with the previously reported systematics.

The data were taken by the E895 Experiment [7] at 2, 4, 6 and 8 AGeV (after correction for energy loss before the target: 1.85, 3.91, 6.0 and 8.0) at the Brookhaven National Laboratory Alternating Gradient Synchrotron (AGS) using the EOS TPC [8]. Global characterization of the collisions is made possible by the nearly 4π center of mass frame coverage provided by this detector. Particle identification is achieved by correlating the average ionization energy loss in the P10 drift gas with the charged particle momenta, reconstructed from the curvature of tracks bent by the Multi-Particle Spectrometer (MPS) magnet as they pass through the TPC.

Secondary tracks are removed from the event samples by removing those tracks which do not originate within 2.5 cm of the reconstructed event vertex. The resulting primary track

charged particle multiplicities are used to establish centrality by assuming a monotonic relationship between impact parameter and multiplicity [9]. Approximately 20,000 of the top 5% most central events, have been selected at each beam energy for this analysis.

Specific details of the particle identification and analysis used to extract the particle spectra are explained in Ref [10], though a short description is included here. The tracks are binned in 0.1 unit rapidity slices from beam to target rapidity, with the mid-rapidity slice corresponding to $|y - y_{cm}| < 0.05$. The transverse mass bins are $25 \text{ MeV}/c^2$ wide in the range $0 < m_t - m_0 < 1.0 \text{ GeV}/c^2$. The mean total momentum and $\beta\gamma$ are computed at the center of the $(m_t - m_0, y)$ bins and are used with a Bethe-Bloch parameterization of the energy loss as a function of $\beta\gamma$ to fit $\langle dE/dx \rangle$ distributions projected from each $(m_t - m_0, y)$ bin.

In certain regions of momentum space, the proton $\langle dE/dx \rangle$ distributions are contaminated by other particle species which must be corrected for in order to extract the proton yields. Pions and kaons are well-separated from the protons in $\langle dE/dx \rangle$ up to a total momentum of approximately $1 \text{ GeV}/c$. Above $1 \text{ GeV}/c$, their particle bands overlap to a degree which makes distinguishing their individual relative yields nearly impossible. Since negative pions comprise the largest fraction of the observed negatively charged particles in this beam energy range, the ratio of oppositely charged pions in the momentum range up to $1 \text{ GeV}/c$ is used to extrapolate to higher momenta. [10] The observed negative pion yields, combined with the extrapolated pion ratios, are used to remove the π^+ contamination from the proton distributions. Kaon contamination is eliminated from the fitting scheme by using the measured kaon results from [11,12] for the same beam energies.

In the particle momentum range between 6 and $8 \text{ GeV}/c$, the proton, deuteron and triton $\langle dE/dx \rangle$ bands significantly overlap, and cannot be resolved. However, above $\sim 8 \text{ GeV}/c$, the expected mean energy loss of these three particles separates again and the proton yields can be extracted. Since the statistics are very limited in this region, the spectra for protons with momenta greater than $\sim 8 \text{ GeV}/c$ have large statistical uncertainties. The result of this three-particle confusion is a broad hole in the final spectra. The $m_t - m_0$ range of the hole varies with the beam energy and rapidity. Where appropriate, the reported errors for the raw proton yields include an estimate of the additional uncertainty resulting from the models used to determine the contamination from other particles.

Simulations of the detector response to protons in all regions of phase space were performed using the GEANT 3.21 simulation package. Small samples (maximum of 4 tracks per event) of proton tracks with momentum distributions approximating the measured data were embedded into raw events. The tagged tracks were propagated through the reconstruction chain along with the raw data. A correction for detector efficiency, acceptance and momentum resolution was obtained from the ratio of found GEANT tracks to the simulated input using the same track quality cuts and centrality selection as the data to be corrected. The proton corrections were largest at very backward rapidities, where detector acceptance causes significant losses, and at forward rapidities and low transverse mass. Forward focussing causes this region to have extremely high track density, which decreases the detection efficiency significantly. However, the corrected spectra, Fig. 1, show very good forward/backward rapidity reflection symmetry.

The transverse mass spectra of the protons in each 0.1 unit rapidity slice at each beam energy are shown in Fig. 1. These spectra have been fit with a static thermal function,

based on the Maxwell-Boltzmann distribution, which does not explicitly include transverse or longitudinal flow.

$$\frac{1}{2\pi m_t} \frac{d^2 N}{dm_t dy} = A(y) m_t e^{-(m_t - m_0)/T(y)}, \quad (1)$$

where $A(y)m_0$ represents the $m_t - m_0 = 0$ intercept and $T(y)$ is the inverse slope parameter. The effect of the chemical potential is contained in $A(y)$. The model agrees fairly well at large $m_t - m_0$, but the agreement deteriorates for very low $m_t - m_0$, where transverse flow modifies Eq. (1). However, the resulting systematic overestimate of the total integrated yields obtained from the fits to the spectra are smaller than the uncertainties in the measured integrated yields, dN/dy .

The rapidity density for purely thermal emission from a stationary source isotropically radiating particles of a given mass can be obtained by integrating over m_t the Maxwell-Boltzmann distribution, Eq. (1), with an overall normalization parameter, B ,

$$\frac{dN_{th}}{dy}(y) = BT^3 \left(\frac{m^2}{T^2} + \frac{m}{T} \frac{2}{\cosh y} + \frac{2}{\cosh^2 y} \right) e^{-\frac{m}{T} \cosh y}. \quad (2)$$

The width of the distribution, Eq. (2), as a function of rapidity for a given emitted particle is a function of the particle mass and temperature only. Using the mid-rapidity inverse slope parameters (determined to an uncertainty of 2 MeV) from the transverse mass spectra fits (Eq. (2)) to approximate the temperature (Table I), this distribution can be compared to the rapidity densities extracted from the integrated transverse mass spectra. The result, shown as the dashed lines in Fig. 2, is clearly too narrow to describe our data.

Schnedermann, Sollfrank and Heinz [1] modeled the increase in the widths as the result of collective longitudinal flow. This assumes that the observed distributions arise from the superposition, in a given rapidity interval, of multiple boosted individual isotropic, locally thermalized sources. This is the longitudinally boost-invariant approach [4] but taken to a finite boost, η_{max} . The distributions are integrated over the source rapidity η to extract the maximum longitudinal flow from the free parameter, η_{max}

$$\frac{dN}{dy} = \int_{\eta_{min}}^{\eta_{max}} d\eta \frac{dN_{th}}{dy}(y - \eta) \quad (3)$$

$$\beta_L = \tanh(\eta_{max}). \quad (4)$$

where $\eta_{max} = -\eta_{min}$, from symmetry about the center of mass; dN_{th}/dy is Eq. (2) with T from Table I; N is the number of protons observed; and β_L is the maximum longitudinal source velocity in units of c .

Fits of this form have been applied to a wide array of experimental data at the AGS and the SPS [1,3,2,13]. Although the inverse slope in Table I is not the true temperature, the longitudinal boost, η_{max} , has been observed to depend only weakly on the temperature input to the model, with the exception of nucleons at SPS energies, which are affected by transparency. [1] In the present data, a 50% decrease in the temperature results in a maximum change of 15% in η_{max} . An average longitudinal flow can be obtained by averaging over η as $\langle \beta_L \rangle = \tanh(\eta_{max}/2)$.

Fits of Eq. (3) to the proton rapidity densities at 2, 4, 6, and 8 AGeV are also shown on Fig. 2. The fit parameter, η_{max} and the corresponding average velocities, $\langle \beta_L \rangle$ are listed in Table I. $\langle \beta \gamma \rangle_L$ is evaluated by computing $\gamma = 1/\sqrt{1 - \langle \beta_L \rangle^2}$.

TABLES

E_{beam} (AGeV)	T_0 (MeV/c ²)	η_{max}	$\langle \beta_L \rangle$	$\langle \beta\gamma \rangle_L$	Ref.
1.06 (Au)	80	0.37	0.19	0.194	
1.15 (Au)	92	0.41	0.20	0.204	[14]
2	187	0.570 ± 0.024	0.28	0.292	
4	211	0.889 ± 0.024	0.42	0.463	
6	216	1.049 ± 0.026	0.48	0.547	
8	229	1.104 ± 0.025	0.50	0.577	
6 (Au)	253	0.990	0.46	0.518	[15]
8 (Au)	267	1.086	0.50	0.577	[15]
10.8 (Au)	279	1.166	0.52	0.609	[15]
11 (Au)	130	1.10	0.50	0.577	[2]
14.6 (Si+Al)	120	1.15	0.52	0.609	[3]
158 (Pb)	160	1.99	0.76	1.169	[2]
200 (S)	220	1.70 ± 0.30	0.69	0.953	[1]

TABLE I. Proton longitudinal Flow parameters extracted from fits of Eq. (3) to the proton rapidity densities at 2, 4, 6, and 8 AGeV, using the mid-rapidity proton inverse slope parameters. Compiled data at other beam energies from the listed references are also included for comparison.

Fig. 3 shows our results for $\langle\beta\gamma\rangle_L$ as a function of beam energy. Also included are the extracted parameters from the compiled data from [1,3,2,13–15].

A modification to a previous interpretation of the lowest energy FOPI data point is presented here. The proton longitudinal flow reported for 1.06 AGeV Au+Au in [2,13,16] is from an interpretation of the measured data from [17] which assumed isotropic emission from a Siemens and Rasmussen [18] radially boosted spherical thermal source. Good agreement between their Au+Au rapidity density distributions and predictions from a Siemens-Rasmussen style model based on fits to their mid-rapidity kinetic energy spectra was reported. [17] A temperature of 80 MeV and an average (isotropic) flow velocity of $\langle\beta_r\rangle = 0.41c$ were reported.

The resulting longitudinal flow velocity of $\langle\beta\rangle = 0.38c$ attributed to the 1.06 AGeV Au+Au data by [2] is a factor of two larger than the value one extracts using the prescription of [1]. In order to make a direct comparison here of the longitudinal flow values at the different beam energies, the same model should be applied in each case. The value reported in Table I and Fig. 3 is from our re-analysis of these FOPI 1.06 AGeV rapidity densities using their reported temperature of 80 MeV with Eq. (3). This model produces an average longitudinal flow of $\langle\beta_L\rangle = 0.19c$, which is consistent with a value obtained using the same model with Au+Au collision data measured by the EOS collaboration at the Bevalac for $E_{beam}=1.15$ AGeV and reported in [14].

The linear systematic trend previously reported [2,13,16] is still evident in the excitation function, but the slope in Fig. 3 has been increased by a factor of ≈ 2.5 to include the present data. The CERN SPS Pb+Pb values no longer show a significant excess above this systematic. The results from 40 AGeV and 80 AGeV Pb+Pb data at the SPS should help to further characterize the systematic trend. In addition, it will be interesting to compare the net proton distributions with the negative hadron or identified particle distributions, to quantify transparency in the transition between the AGS and the top energy SPS. Within the model [1] used here, all of the heaviest systems (Au+Au and Pb+Pb) have a nearly linear longitudinal flow velocity, $\langle\beta\gamma\rangle_L$, versus $\log(E_{beam})$.

This work was supported in part by the US National Science Foundation under Grants No. PHY-98-04672, PHY-9722653, PHY-96-05207, PHY-9601271, and PHY-9225096; by the U.S. Department of Energy under grants DE-FG02-87ER40331.A008, DE-FG02-89ER40531, DE-FG02-88ER40408, DE-FG02-87ER40324, and contracts DE-AC03-76SF00098, DE-AC02-98CH10886; and by the University of Auckland Research Committee, NZ/USA Co-operative Science Programme CSP 95/33; and by the National Natural Science Foundation of P.R. China under grant number 19875012.

FIGURES

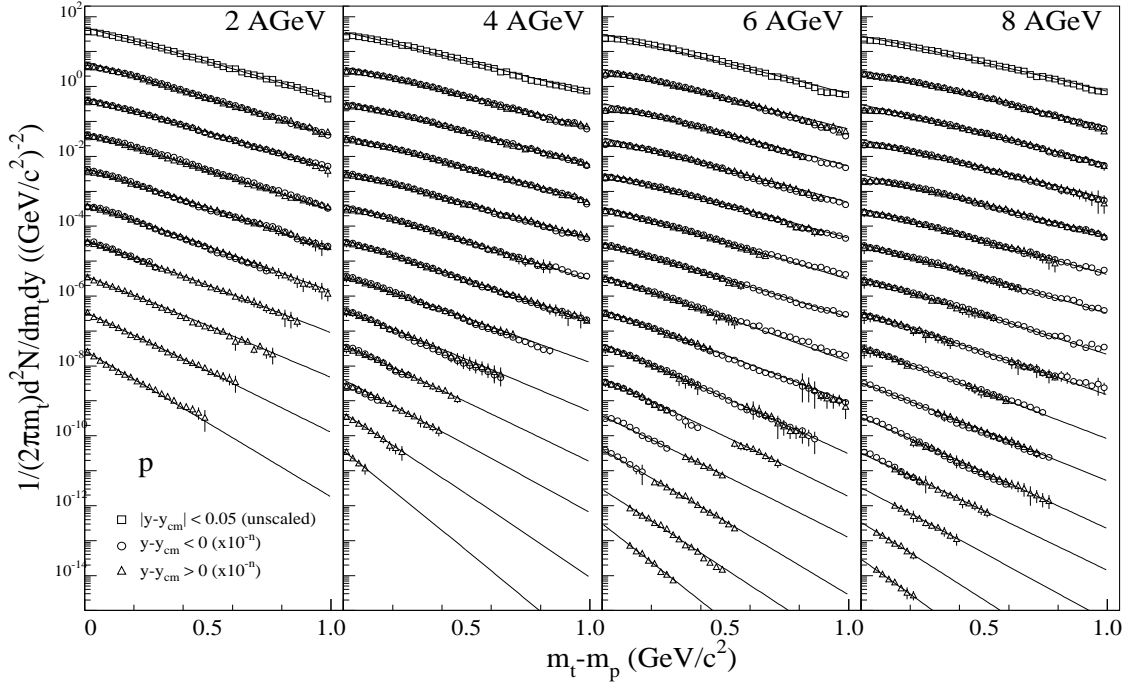


FIG. 1. Invariant yield per event as a function of $m_t - m_p$ for protons at 2, 4, 6, and 8 AGeV. Midrapidity is shown unscaled, while the 0.1 unit forward/backward rapidity slices are scaled down by successive factors of 10.

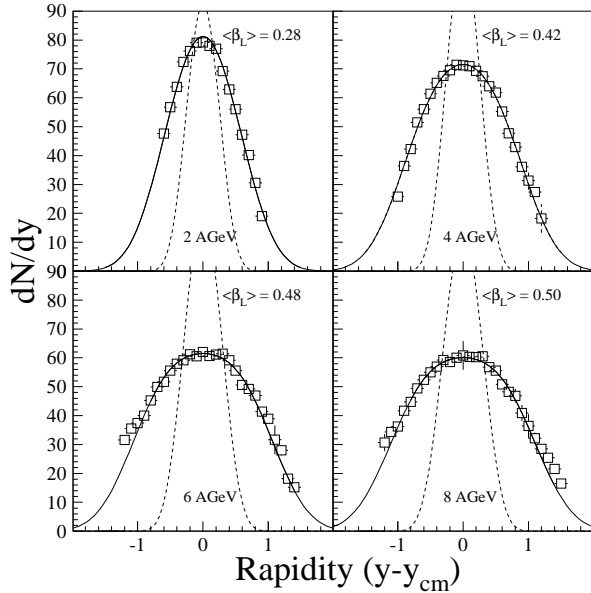


FIG. 2. Proton rapidity density distributions at 2, 4, 6, and 8 AGeV. The dashed curves indicate the expectation for isotropic emission from a stationary thermal source with temperatures given by the inverse slope parameters from the transverse mass fits (Eq. (2)), whereas the solid curves indicate fits with longitudinal flow (Eq. (3)).

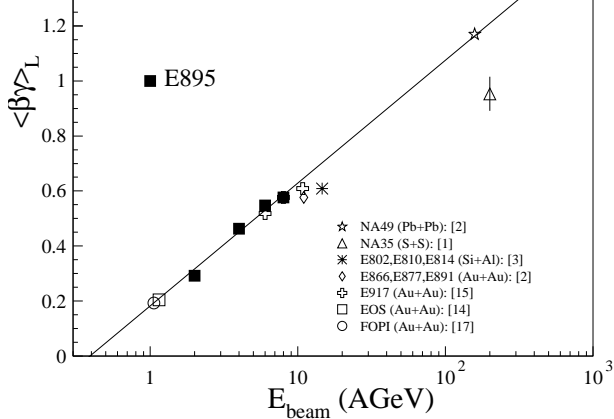


FIG. 3. Energy excitation function of longitudinal flow velocities ($\langle \beta \gamma \rangle_L$), from heavy ion collisions. The open circle has been adjusted here as described in the text. A roughly linear dependence for heavy systems over more than two orders of magnitude of beam energy is illustrated.

REFERENCES

- [1] E. Schnedermann, J. Sollfrank and U. Heinz, Phys. Rev. C **48**, 2462 (1993).
- [2] J. Stachel, Nucl. Phys. A **610**, 509c (1996).
- [3] P. Braun-Munzinger, J. Stachel, J.P. Wessels, N. Xu, Phys. Lett. B **344**, 43 (1995).
- [4] J.D. Bjorken, Phys. Rev. D **27**, 140 (1983).
- [5] H. Appelshäuser, *et al.*, (NA49 Collaboration), Phys. Rev. Lett. **82**, 2471 (1999).
- [6] Harald Dobler, Josef Sollfrank, Ulrich Heinz, Phys. Lett. B **457**, 353 (1999).
- [7] G. Rai, *et al.*, LBL-PUB-5399 (1993).
- [8] H. Wieman, *et al.*, Nucl. Phys. **A525**, 617c (1991).
- [9] C. Cavata, *et al.*, Phys. Rev. C **42**, 1760 (1990).
- [10] J.L. Klay, Ph.D. Dissertation, University of California, Davis (2001).
- [11] C.A. Ogilvie, Nucl. Phys. A **638**, 57c (1998).
- [12] J.C. Dunlop, Ph.D. Dissertation, Massachusetts Institute of Technology (1999).
- [13] Norbert Herrmann, Johannes P. Wessels, and Thomas Wienold, Annu. Rev. Nucl. Part. Sci. **49**, 581 (1999).
- [14] H. Liu, *et al.*, (E895 Collaboration), Nucl. Phys. A **630**, 549c (1998).
- [15] B.B. Back, *et al.* (E917 Collaboration), Phys. Rev. Lett. **86**, 1970 (2001).
- [16] J.P. Wessels, *Flow Phenomena at AGS Energies*, Talk at the Workshop 'QCD Phase Transitions', Hirscheegg, Austria, January 13-18, 1997 (Available at the Los Alamos pre-print server: <http://xxx.lanl.gov/ps/nucl-ex/9704004>).
- [17] N. Herrmann, (FOPI Collaboration), Nuc. Phys. **A610**, 49c (1996).
- [18] P.J. Siemens and J.O. Rasmussen, Phys. Rev. Lett. **42**, 880 (1979).